

3D Modelling of Twist Wall at the Electrode Edge of Liquid Crystal Cells

Zijun Nie, Mengyang Yang, Eero Willman, F. Anibal Fernández, Sally E. Day

University College London, Torrington Place, London, WC1E 7JE, U.K.

Abstract

Q-tensor simulation of the liquid crystal structure at the edge of electrodes has been carried out. The modeling shows a twist wall, which reverses direction to form a zig-zag structure. The results are compared with experiment. Also a defect loop is found in micro-lenses formed using a hole electrode structure.

Keywords

Modeling; liquid crystal; twist wall; defects.

1. Introduction

The structure of the liquid crystal (LC) director at the edge of an electrode with planar alignment is investigated in this paper. Results for a thin layer ($0.5\ \mu\text{m}$) have already been presented in [1], where a defect pair was obtained on one side of an electrode edge. In contrast, a thick layer LC device has been observed in the laboratory using a microscope (Figure 1). At the edge of one side of the electrode, a zig-zag line is visible experimentally. This has been simulated by director modeling together with calculation of the optical properties, allowing comparison with experiment.

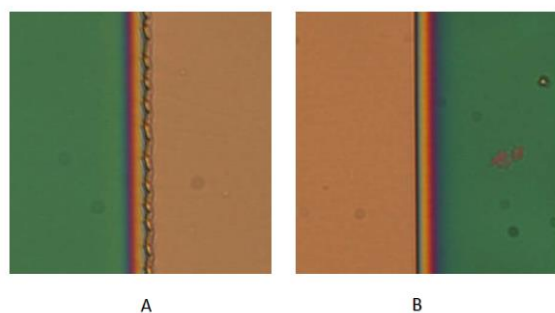


Figure 1. Micrograph of electrode edges using white light, 50x lens with Nikon's Eclipse polarizing microscope (A) left edge (B) right edge, parallel polarizer at 45° to rubbing direction.

A diagram of the structure is shown in Figure 2. The unchanged pre-tilt at the substrate surfaces in Figure 2 is defined as a positive angle of pre-tilt in the modelling. Side A has a conflict between the pre-tilt and direction of the electric field from the edge of the electrode, shown in the red circle. This was shown previously to give rise to defect lines in the thin cell [1].

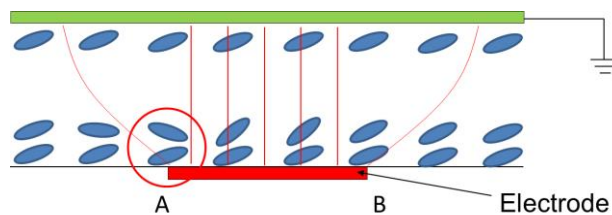


Figure 2. Model of electrode with pre-tilt alignment

The same methods have also been used to investigate liquid crystal microlenses. Modelling of LC microlenses can be used to improve

the performance for particular applications. One type of lens structure has been considered in this paper, which is formed using a hole in the electrode. A defect loop is found in this case.

2. Background

Modeling of liquid crystals has been useful since the start of their application in displays [2] to optimize the parameters and structure of displays. This paper presents results of modelling LC structures at the edges of electrodes for planar aligned devices which are used as phase modulators for beam steering and diffractive elements. The modelling can be useful in understanding the LC structures and allows many parameters to be varied in a way that is difficult experimentally, particularly for devices such as liquid crystal on silicon (LCOS) which are expensive to make as prototypes.

Modeling in 2D has been useful, but is not always enough because even at long electrode edges, 3D defect structures are sometimes found, for example, the type shown in Figure 1A. Simulation methods are available now and allow modeling of 3D structures, including defect formation [3]. Q-tensor liquid crystal modelling programs developed at UCL have been used to calculate the LC structure and defect formation in high resolution liquid crystal devices [4].

3. Structure for Modelling

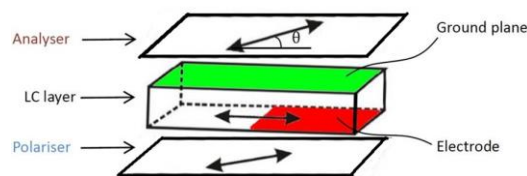


Figure 3. Structure of the 3D model

The model for the edge of the electrode, shown in Figure 3, is a LC cell with a half electrode at the bottom and with a ground plane on the top surface. Two values of liquid crystal layer thickness were modeled, $4.5\ \mu\text{m}$ and $10\ \mu\text{m}$. The optical modeling used two polarizers at $\theta = 45^\circ$ to the rubbing direction.

For the director modelling, boundary conditions must be defined on the sides of the region to be modeled. In this case we assume the LC layer continues in the cell plane, so Neumann conditions on these boundaries are used. The surface alignment at the top and bottom of the cell has a pre-tilt angle of $+2^\circ$. The upper electrode (green) is taken as ground. The red electrode has 10 V applied. The LC material used in the experiments was E7 [2] and the material constants used in the simulation are given in Table 1.

Table 1. Material parameters of simulation [5].

Elastic constant	Dielectric & viscosity		Thermal constants		
	k_{11}	ϵ_{\parallel}	ϵ_{\perp}	A	B
k_{11}	11.7pN	ϵ_{\parallel}	19.5	A	0
k_{22}	8.8pN	ϵ_{\perp}	5.17	B	2.13×10^5
k_{33}	19.5pN	γ_1	0.190	C	1.73×10^5

4. Results

4.1 Twist Wall Defect

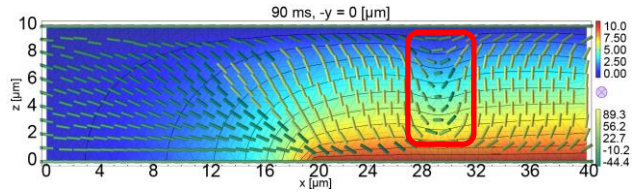


Figure 4. Twist wall defect at the cross section of $y = 0 \mu\text{m}$. Background color represents the potential, rods indicates orientation of LC director.

Initial results were obtained for a cell gap of $z = 10 \mu\text{m}$. The modeling was for a 3D structure and the size in the other directions were $x = 40 \mu\text{m}$, $y = 40 \mu\text{m}$. The result shown in Figure 4 is the xz -cross section at $y = 0 \mu\text{m}$. A twist wall defect was found, shown in the red circle above the electrode area.

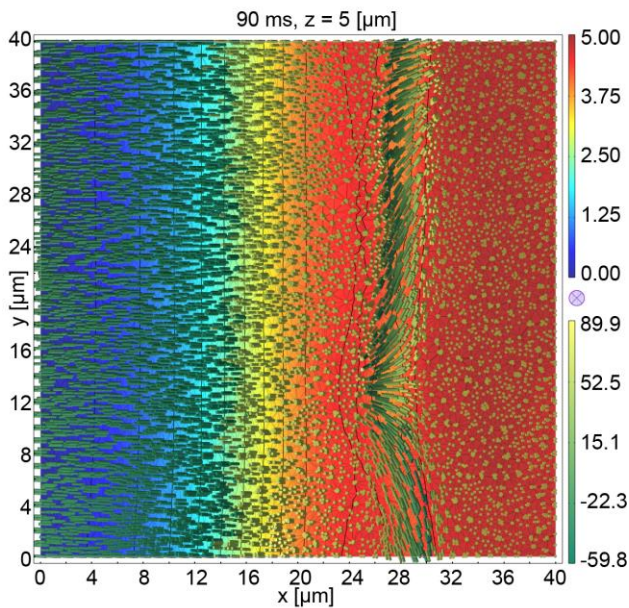


Figure 5. The top view of Zig-zag Line at the cross section of $z = 5 \mu\text{m}$.

The background color shows the electric potential. The color of director rods indicates tilt angle to the surface of the cell. The director field is continuous in the Q-tensor simulation, although extracting the director angles for plotting has resulted in an abrupt change in tilt, where the twist has also changed abruptly, as seen by the color change in the region between $x = 20$ and $x = 12$. Figure 5 shows a top view, cross section through the center, at $z = 5 \mu\text{m}$.

The twist wall of the LCs is seen at $x = 30 \mu\text{m}$ and it has a zig-zag form with a change in the director twist at $y = 14 \mu\text{m}$. The disclination shown in Figure 4 is an S Wall, as classified by A. Stieb [6]. Comparison of the simulation with the experimental results in Figure 1 shows a shorter distance between the twist wall reversal, or zig-zag.

The exact shape of the defect observed experimentally is likely to be strongly dependent of inhomogeneity and imperfections of the cell structure, including surface treatment and geometry. This is also supported by the fact that different cells show slightly different shapes of the disclinations. Only one kink over $40 \mu\text{m}$ is seen in the

simulation of the $10 \mu\text{m}$ cell gap, so there are some differences from the experimental results. In order obtain a correct comparison, the cell gap was measured.

4.2 Accurate thickness

An accurate measurement of the thickness of the LC cell sample was found using a spectrophotometer. A region containing an air gap in the cell was used to obtain the visible transmission spectrum, which shows Fabry-Perot fringes related to the spacing. The spacing of the fringes (free spectral range, FSR) has been plotted as a function of the wavelength of the fringe.

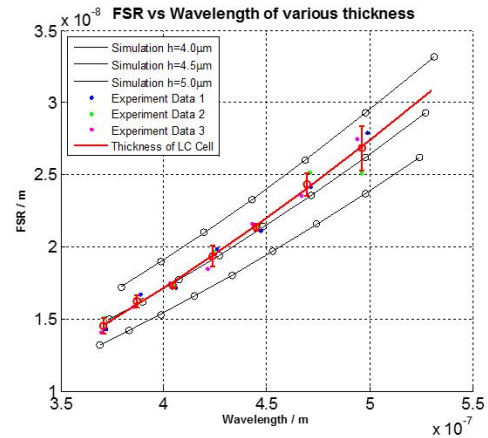


Figure 6. Fringe spacing (FSR) as a function of wavelength for the LC cell, showing measured and calculated values.

The simulation results of fringe spacing with wavelength from $4.0 \mu\text{m}$ to $5.0 \mu\text{m}$ are shown in black lines in Figure 6. The mean and standard deviation of the experimental data are represented as the red line with error bars. Hence, the thickness of LC cell is found to be $4.5 \pm 0.1 \mu\text{m}$. This thickness value was used for the next set of simulations.

4.3 Director modelling

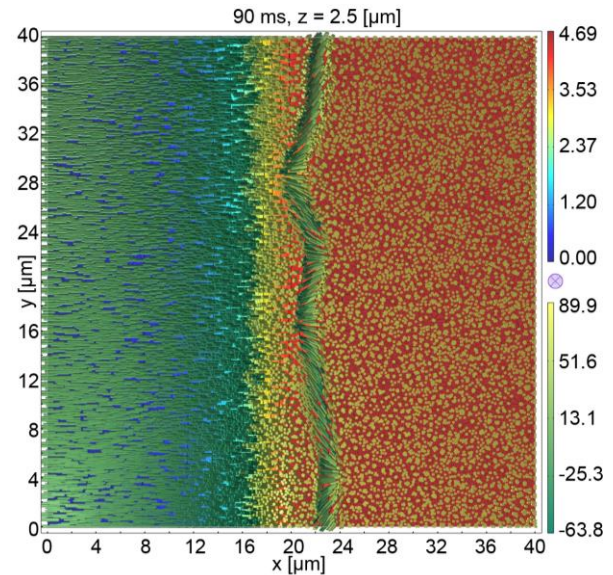


Figure 7. Simulation of $4.5 \mu\text{m}$ cell and director profile at $z = 2.5 \mu\text{m}$

Figure 7 shows the director modelling for the 4.5 μm thickness at 90 ms after a 10 V voltage was applied to the electrode. The background is shown as the potential at $z = 2.5 \mu\text{m}$, so the color bar is from 0 – 4.69 V. The color on the cylinders represents the tilt angle.

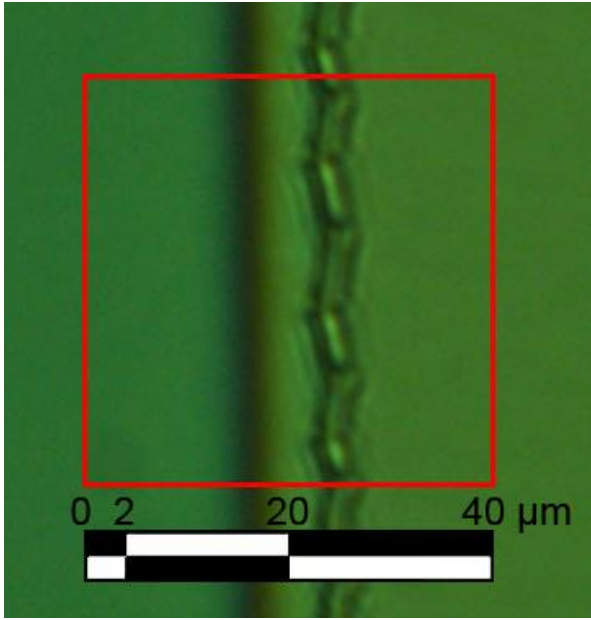


Figure 8. Optical micrograph of side A of the cell, using a green narrow band filter, showing a 40 μm square.

Figure 8 shows the experiment result for the 4.5 μm thick cell with parallel polarizers at 45° to the rubbing direction and with 6 V applied voltage. A green optical filter (550 nm narrow band filter) was used in the illumination. The length scale is shown.

The simulation and experiment show qualitative agreement because the shape and the number of kinks is similar between them. Further work is needed to calculate the optical properties found in the experiment, where the incident light is not fully collimated by the microscope illumination.

4.4 Surface relief

Some surface relief may be present in the experimental cell, due to the electrode thickness, so a simulation including a 0.1 μm sloping step is shown in Figure 9.

It was found that the zig-zag defect form is similar to the case of the planar structure and the position of the defect at the same position from the edge of the electrode.

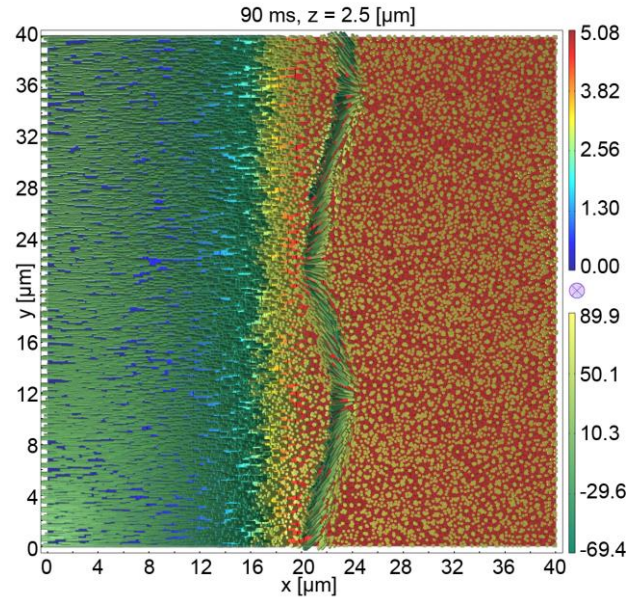


Figure 9. Director profile at $z = 2.5 \mu\text{m}$, with a 0.1 μm step at the electrode edge.

5. Microlenses

The LC lens concept was first published in 1979 by Susumu Sato [7]. LC lenses can be categorized according to the method of focus: either refraction or diffraction. The refraction LC lenses act as gradient refractive index (GRIN) lenses. The hole-patterned electrode structure is often formed by one or two asymmetric holes in top or bottom electrode [8].

The structure relies on the fringing fields at the edge of the circular electrode. As a result, this is an interesting structure to study in the context of defect formation. We have modeled, in 3D, a 35 μm thick cell with a hole in the electrode on one side of radius $r = 100 \mu\text{m}$.

The size of this simulation is $x = 200 \mu\text{m}$, $y = 200 \mu\text{m}$, and cell gap, $z = 35 \mu\text{m}$. The director profile is shown in section in Figure 10 and in plan in Figure 11. The results show a circular line defect, but no evidence of the twist wall and the line defect pair is displaced in the x - y plane.

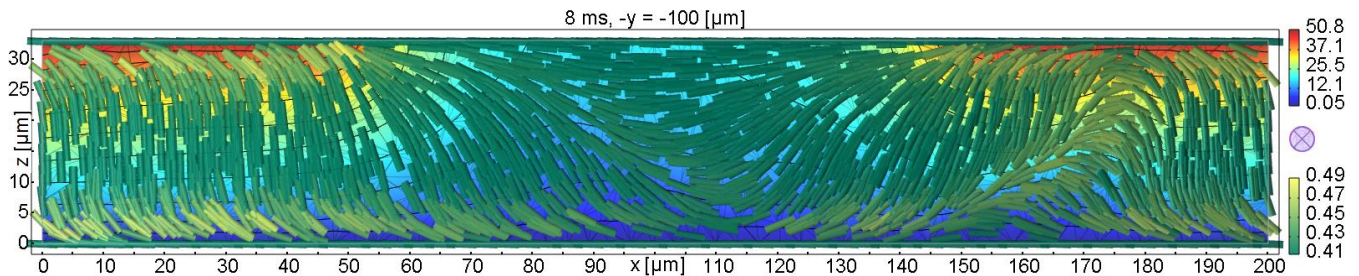


Figure 10. Director result for hole-patterned electrode

Figure 11 shows the top view of hole structure at $z = 25 \mu\text{m}$ where the background color is electric potential. The color of director rods indicates the order parameter of the liquid crystal. The twist wall can be seen to the right of the Figure. The wall then forms across the aperture at the substrate level to complete the loop.

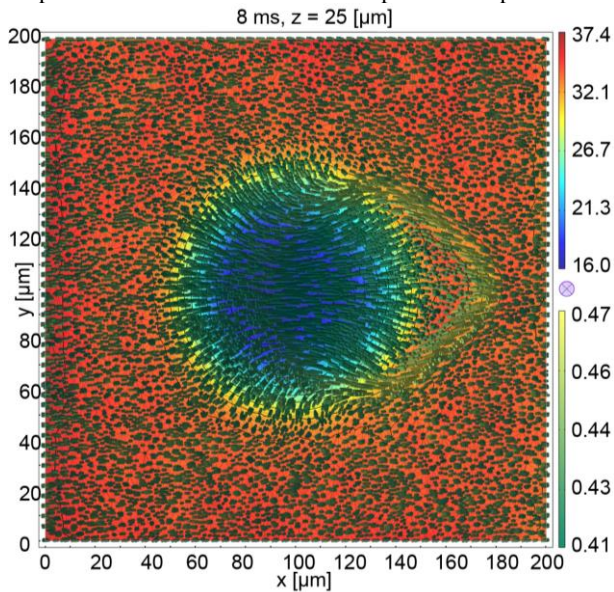


Figure 11. The top view of hole-patterned electrode at $z = 25 \mu\text{m}$

6. Conclusion

The 3D modelling of liquid crystal at the edge of an electrode is investigated. The twist wall defect is formed at the edge structure for a long straight electrode. It was found that the cell gap has an effect on the length of zig-zag and qualitative agreement with experiment was found. A line-loop defect is simulated in a microlens formed using a hole electrode.

7. References

- [1] Z. Nie, S. E. Day, F. A. Fernández, E. Willman, and R. James, "P-105 Modelling of Liquid Crystals at the Pixel Edge, SID Symposium Digest of Technical Papers Volume 45, Issue 1," *SID Symposium Digest of Technical Papers*, vol. 45, pp. 1382-1385, 01 2014.
- [2] D. W. Berreman, "Numerical Modeling of Twisted Nematic Devices," *Philosophical Transactions of the Royal Society A-Mathematical Physical and Engineering Sciences*, vol. 309, pp. 203-216, 1983.
- [3] R. James, E. Willman, F. A. Fernandez, and S. E. Day, "Finite-element modeling of liquid-crystal hydrodynamics with a variable degree of order," *IEEE Transactions on Electron Devices*, vol. 53, pp. 1575-1582, 2006.
- [4] E. Willman, F. A. Fernandez, R. James, and S. E. Day, "Modeling of weak anisotropic anchoring of nematic liquid crystals in the Landau-de Gennes theory," *IEEE Transactions on Electron Devices*, vol. 54, pp. 2630-2637, Oct 2007.
- [5] J. Li, G. Baird, Y. H. Lin, H. W. Ren, and S. T. Wu, "Refractive-index matching between liquid crystals and photopolymers," *Journal of the Society for Information Display*, vol. 13, pp. 1017-1026, Dec 2005.
- [6] A. Stieb, G. Baur, and G. Meier, "Alignment Inversion Walls in Nematic Liquid Crystal Layers Deformed by an Electric Field," *J. Phys. Colloques*, vol. 36, pp. C1-185-C1-188, 1975.
- [7] S. Sato, "Liquid-Crystal Lens-Cells with Variable Focal Length," *Japanese Journal of Applied Physics*, vol. 18, pp. 1679-1684, 1979.
- [8] L. G. Commander, S. E. Day, and D. R. Selviah, "Variable focal length microlenses," *Optics Communications*, vol. 177, pp. 157-170, Apr 15 2000.